

General one-loop contributions to the decay $H \rightarrow \nu_l \bar{\nu}_l \gamma$

Khiem Hong Phan^{1,2}, Dzung Tri Tran³, and Le Tho Hue⁴

¹⁾*Institute of Fundamental and Applied Sciences, Duy Tan University, Ho Chi Minh City 700000, Vietnam*

²⁾*Faculty of Natural Sciences, Duy Tan University, Da Nang City 550000, Vietnam*

³⁾*University of Science Ho Chi Minh City, 227 Nguyen Van Cu, District 5, HCM City, Vietnam*

⁴⁾*Institute of Physics, Vietnam Academy of Science and Technology, 10 Dao Tan, Ba Dinh, Hanoi, Vietnam*

Abstract

General one-loop contributions to the decay amplitudes $H \rightarrow \nu_l \bar{\nu}_l \gamma$ are presented, considering all possible contributions of additional heavy vector gauge bosons, fermions, and charged (and also neutral) scalar particles appearing in the loop diagrams. Moreover, the results can be applied directly when extra neutrinos (apart from three ones in standard model) are taken into account in final states. Analytic results are presented in terms of Passarino-Veltman scalar functions which can be evaluated numerically using `LoopTools`. In the standard model framework, these analytical results are generated and cross-checked with previous computations. We find that our results are well consistent with these computations. Within standard model limit, phenomenological results for the decay channels are also studied using the updated input parameters at the Large Hadron Collider.

Keywords: Higgs phenomenology, one-loop corrections, analytic methods for quantum field theory, dimensional regularization.

1. Introduction

Searching for all decay modes of the standard model-like (SM-like) Higgs boson are one of the main purposes at the High Luminosity Large Hadron Collider (HL-LHC) [1, 2] as well as Future Lepton Colliders [3]. Because the partial decay widths of Higgs boson contain an important information for testing the nature of Higgs sector. Among the Higgs decay modes, the channels of $H \rightarrow$ invisible particles [4, 5, 6, 7, 8, 9, 10] and $H \rightarrow \gamma$ plus invisible particles [11, 12] are great of interest by following reasons. First, these decay processes can be measured at the LHC [4, 5, 6, 8, 11, 12]. Therefore, they could be used for verifying the standard model at higher energy regions. On the other hands, there are exist many models beyond the standard model (BSM) in which new invisible particles rather than neutrinos are proposed. In addition, many new heavy particles that are absent in SM may exchange in the loop diagrams of the aforementioned decay channels. The leading contributions to the decays $H \rightarrow \nu_l \bar{\nu}_l \gamma$ are from one-loop level without diagrams containing photon exchanges. The decay rates will be more sensitive with new contributions from BSMs than those of the decays $H \rightarrow e^+ e^- \gamma, \mu^+ \mu^- \gamma$, which consist of both tree contributions from Yukawa coupling $H l \bar{l}$ and one loop contributions from photon exchange [22, 23, 24]. With the latest experimental report, evidence of these two decay channels have been concerned at 3.2σ over background and $m_u < 30$ GeV [25]. Correspondingly, the contributions from Z exchanges do not appear in this observation, but CMS collaboration has been searching for them through the channels $H \rightarrow Z \gamma \rightarrow l \bar{l} \gamma$ [26], which may have the same properties as the decays $H \rightarrow \nu_l \bar{\nu}_l \gamma$ in the SM framework. As a result, the decay widths of $H \rightarrow \nu_l \bar{\nu}_l \gamma$ could provide an useful tool for controlling SM background as well as constraining new physics parameters.

One-loop formulas for $H \rightarrow \nu_l \bar{\nu}_l \gamma$ within SM framework have computed in Ref. [13]. Besides that, a model independent for investigating Higgs decay to a photon and invisible particles has been proposed in Ref. [14]. The decay channel of Higgs to a photon and light vector gauge bosons which they belong to $U(1)$ extension of SM has also considered in Ref. [15]. In next-to-minimal supersymmetry (SUSY) framework, Higgs decay to photon plus pair of lightest susy particles have studied in Ref. [16]. In Ref. [16], the decay process has been used for probing dark matter as well as constraining SUSY parameters. Supersymmetry-breaking scale has been examined through the Higgs decay to photon and gravitinos in [17].

In this article, we present general one-loop formulas for the decay $H \rightarrow \nu_l \bar{\nu}_l \gamma$. The results are valid for many BSMs which new heavy vector bosons, fermions, and scalar particles predicted by these models are considered in the loop diagrams. Moreover, the calculations can be extended directly when the extra neutrinos (rather than 3 in standard model) are taken into account in final states. Analytic results are presented in terms of Passarino-Veltman scalar functions which can be computed numerically by using the package `LoopTools`. The calculations are also verified numerically by checking the ultraviolet finiteness of the results. We find that the results are good stability when varying ultraviolet cutoff parameters. The results are then applied to the case of standard model which the decay rates are generated and cross-checked with the previous computations. Our results in this work are good agreement with the previous references. All physical results for the decay channels within SM are examined with taking updated input parameters at the Large Hadron Collider. While the phenomenological results for the decay processes in several BSMs are referred to our next papers.

The results of this work can be applied calculate one-loop contributions of new particles predicted by well-known BSM constructed previously, for examples many popular SM extensions including only new charged scalars such as two Higgs doublet models. In the SUSY model, new loop contributions come from charged Higgs bosons, superpartners of leptons and gauge bosons. One loop contribution from new charged gauge bosons may appear in many electroweak gauge extensions such as the left-right models (LR) constructed from the $SU(2)_L \times SU(2)_R \times U(1)_Y$ [27, 28, 29], the 3-3-1 models ($SU(3)_L \times U(1)_X$) [30, 31, 32, 33, 34, 35, 36], the 3-4-1 models ($SU(4)_L \times U(1)_X$) [36, 37, 38, 39, 40, 41], ect. These one-loop contributions may be significant in the amplitudes of the mentioned decay processes. Phenomenological results for the decay processes in the mentions models will be very interesting for further studies, which will be our future projects.

The layout of the paper is as follows: In section 2, we present briefly one-loop tensor reduction method. Detailed calculations for one-loop contributions to $H \rightarrow \nu_l \bar{\nu}_l \gamma$ are presented in this section. Conclusions and outlook are devoted in section 3. In appendices, Feynman rules and involving couplings in the decay processes are shown.

2. Calculation

Detailed calculations for one-loop contributions to $H \rightarrow \nu_l \bar{\nu}_l \gamma$ are presented in this section. We first describe briefly one-loop tensor reduction method in the following subsection. General analytic results and physical results of the decay processes are then shown in the next subsections.

2.1. Method

In this calculation, we follow tensor reduction method developed in Ref. [18]. Following the technique, tensor one-loop integrals with N -external lines can be decomposed into scalar functions with $N \leq 4$. The approach will be explained briefly in the following paragraphs.

First, one-loop one-, two-, three- and four-point tensor integrals with rank P are defined:

$$\{A; B; C; D\}^{\mu_1 \mu_2 \dots \mu_P} = (\mu^2)^{2-d/2} \int \frac{d^d k}{(2\pi)^d} \frac{k^{\mu_1} k^{\mu_2} \dots k^{\mu_P}}{\{D_1; D_1 D_2; D_1 D_2 D_3; D_1 D_2 D_3 D_4\}}. \quad (1)$$

In this formula, D_j ($j = 1, \dots, 4$) are the inverse Feynman propagators

$$D_j = (k + q_j)^2 - m_j^2 + i\rho, \quad (2)$$

$q_j = \sum_{i=1}^j p_i$, p_i are the external momenta, and m_j are internal masses in the loops. We are working on space-time dimension $d = 4 - 2\varepsilon$. The parameter μ^2 plays role of a renormalization scale. We then present explicit reduction formulas for one-loop one-, two-, three- and four-point tensor integrals up to rank $P = 3$ as follows [18]:

$$A^\mu = 0, \quad (3)$$

$$A^{\mu\nu} = g^{\mu\nu} A_{00}, \quad (4)$$

$$A^{\mu\nu\rho} = 0, \quad (5)$$

$$B^\mu = q^\mu B_1, \quad (6)$$

$$B^{\mu\nu} = g^{\mu\nu} B_{00} + q^\mu q^\nu B_{11}, \quad (7)$$

$$B^{\mu\nu\rho} = \{g, q\}^{\mu\nu\rho} B_{001} + q^\mu q^\nu q^\rho B_{111}, \quad (8)$$

$$C^\mu = q_1^\mu C_1 + q_2^\mu C_2 = \sum_{i=1}^2 q_i^\mu C_i, \quad (9)$$

$$C^{\mu\nu} = g^{\mu\nu} C_{00} + \sum_{i,j=1}^2 q_i^\mu q_j^\nu C_{ij}, \quad (10)$$

$$C^{\mu\nu\rho} = \sum_{i=1}^2 \{g, q_i\}^{\mu\nu\rho} C_{00i} + \sum_{i,j,k=1}^2 q_i^\mu q_j^\nu q_k^\rho C_{ijk}, \quad (11)$$

$$D^\mu = q_1^\mu D_1 + q_2^\mu D_2 + q_3^\mu D_3 = \sum_{i=1}^3 q_i^\mu D_i, \quad (12)$$

$$D^{\mu\nu} = g^{\mu\nu} D_{00} + \sum_{i,j=1}^3 q_i^\mu q_j^\nu D_{ij}, \quad (13)$$

$$D^{\mu\nu\rho} = \sum_{i=1}^3 \{g, q_i\}^{\mu\nu\rho} D_{00i} + \sum_{i,j,k=1}^3 q_i^\mu q_j^\nu q_k^\rho D_{ijk}. \quad (14)$$

The short notation [18] $\{g, q_i\}^{\mu\nu\rho}$ is used as follows: $\{g, q_i\}^{\mu\nu\rho} = g^{\mu\nu} q_i^\rho + g^{\nu\rho} q_i^\mu + g^{\mu\rho} q_i^\nu$ in the above relations. The scalar coefficients $A_{00}, B_1, \dots, D_{333}$ in the right hand sides of the above equations are so-called Passarino-Veltman functions (PV) [18]. Analytic formulas of the PV functions are well-known and they have been implemented into **LoopTools** [20] for numerical computations.

2.2. General one-loop contributions to $H \rightarrow \nu_l \bar{\nu}_l \gamma$

General one-loop contributions to $H(p) \rightarrow \nu_l(q_1) \bar{\nu}_l(q_2) \gamma(q_3)$ in arbitrary beyond the standard models are calculated in this section. One-loop Feynman diagrams involving the decay processes can be grouped into several classes shown in the following paragraphs. For on-shell external photon, the ward identity is implied. As a result, we apply the following relation: $q_3^\nu \epsilon_\nu^* = 0$ where

q_3^ν , ϵ_ν^* are momentum and polarization vector of the external photon respectively. Kinematic invariant variables involving to the decay processes are included:

$$\begin{aligned} p^2 &= M_H^2, \quad q_1^2 = q_2^2 = q_3^2 = 0, \\ q_{12} &= q^2 = (q_1 + q_2)^2 = 2q_1 \cdot q_2, \quad q_{13} = 2q_1 \cdot q_3, \quad q_{23} = 2q_2 \cdot q_3. \end{aligned} \quad (15)$$

The general one-loop amplitude which obeys the invariant Lorentz structure can be decomposed as follows [24]:

$$\mathcal{A}_{\text{loop}} = \sum_{k=1}^2 \left\{ [q_3^\mu q_i^\nu - g^{\mu\nu} q_3 \cdot q_k] \bar{u}(q_1) (F_{k,R} \gamma_\mu P_R + F_{k,L} \gamma_\mu P_L) v(q_2) \right\} \epsilon_\nu^*. \quad (16)$$

In this equation, all form factors are computed as follows:

$$F_{k,L/R} = F_{k,L/R}^{\text{Trig}} + F_{k,L/R}^{\text{Box}} \quad (17)$$

for $k = 1, 2$. Each form factor in (16) will be contributed from different kind of particles such as vector bosons V_i , charged scalar particles S_i and fermions f_i exchanging in loop diagrams. These particles appear in many BSMs whose the Feynman rules are collected in Tables B.4 and B.5. After using them to write down all one-loop contributions to the decay amplitudes, the **Package-X** [19] will be used to contract all Dirac traces in the general dimension d . The analytic formulas of all one-loop contributions will be then decomposed into one-loop tensor integrals. In this step, the above tensor reduction method is employed to transform all tensor integrals into scalar functions included in the form factors $F_{k,L/R}$. Finally, they are collected as functions of the well-known Passarino-Veltman scalar coefficients [18, 20].

2.2.1. One-loop triangle diagrams

We are going to present the calculation in detail. We first arrive at the contributions of one-loop triangle diagrams with exchanging vector bosons V_i, V_j in loop (seen Fig. 1).

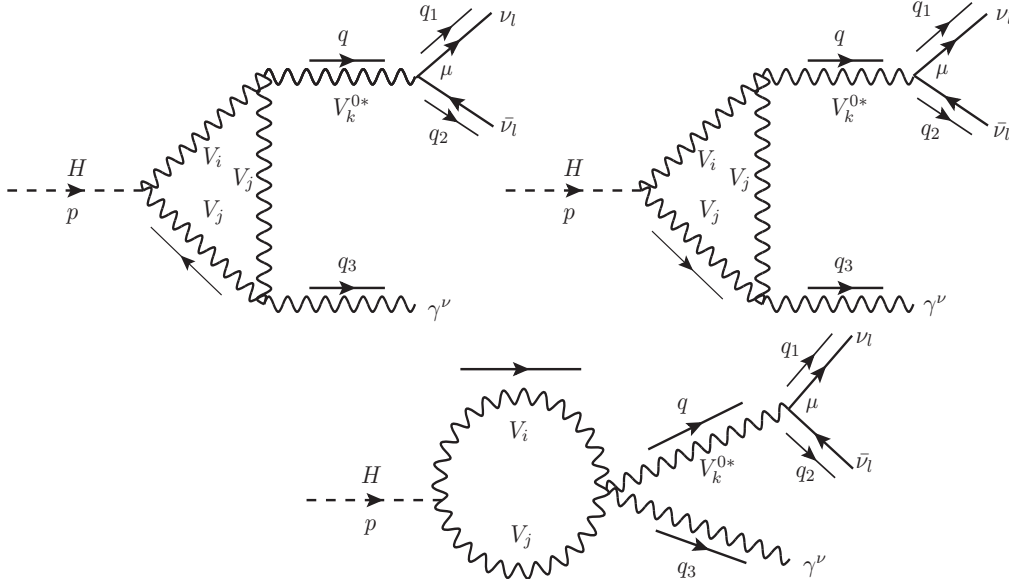


Figure 1: One-loop triangle diagrams with exchanging vector bosons $V_{i,j}$ particles in loop.

By applying one-loop tensor reduction method in the previous subsection, the form factors are expressed in terms of PV-functions as follows:

$$\begin{aligned}
F_{k,L}^{\text{Trig}}|_{V_i, V_j} = & \sum_{V_i, V_j} \frac{g_{HV_i V_j} g_{V_k^0 \nu_l \bar{\nu}_l}^L}{32\pi^2 M_{V_i}^2 M_{V_j}^2 (q^2 - M_{V_k^0}^2 + i\Gamma_{V_k^0} M_{V_k^0})} \times \\
& \times \left\{ \left[eQ g_{V_k^0 V_i V_j} (M_H^2 + M_{V_i}^2 + M_{V_j}^2) + 2g_{V_k^0 A V_i V_j} (M_H^2 - M_{V_i}^2) \right] B_{11}(M_H^2, M_{V_j}^2, M_{V_i}^2) \right. \\
& + \left[eQ g_{V_k^0 V_i V_j} (M_H^2 - M_{V_i}^2 + 3M_{V_j}^2) - 2g_{V_k^0 A V_i V_j} M_{V_j}^2 \right] B_1(M_H^2, M_{V_j}^2, M_{V_i}^2) \\
& + 2M_{V_j}^2 \left[eQ g_{V_k^0 V_i V_j} - g_{V_k^0 A V_i V_j} \right] B_0(M_H^2, M_{V_j}^2, M_{V_i}^2) \\
& + 2g_{V_k^0 A V_i V_j} \left[M_H^2 B_{111} + B_{00} + 2B_{001} \right] (M_H^2, M_{V_j}^2, M_{V_i}^2) \\
& + 4eQ g_{V_k^0 V_i V_j} M_{V_j}^2 \left(3M_{V_i}^2 + M_{V_j}^2 - q^2 \right) C_0(0, q^2, M_H^2, M_{V_j}^2, M_{V_i}^2, M_{V_i}^2) \\
& + 2eQ g_{V_k^0 V_i V_j} \left[M_H^2 (M_{V_i}^2 + M_{V_j}^2 - q^2) + (4d - 6) M_{V_i}^2 M_{V_j}^2 + M_{V_i}^4 + M_{V_j}^4 \right. \\
& \quad \left. - q^2 (M_{V_i}^2 + M_{V_j}^2) \right] (C_{22} + C_{12})(0, q^2, M_H^2, M_{V_j}^2, M_{V_i}^2, M_{V_i}^2) \\
& + 2eQ g_{V_k^0 V_i V_j} \left[M_H^2 (M_{V_i}^2 + M_{V_j}^2 - q^2) + (4d - 6) M_{V_i}^2 M_{V_j}^2 + 3M_{V_j}^4 \right. \\
& \quad \left. - M_{V_i}^4 + q^2 (M_{V_i}^2 - 3M_{V_j}^2) \right] C_2(0, q^2, M_H^2, M_{V_j}^2, M_{V_j}^2, M_{V_i}^2) \left. \right\}, \tag{18}
\end{aligned}$$

$$F_{k,R}^{\text{Trig}}|_{V_i, V_j} = F_{k,L}^{\text{Trig}}|_{V_i, V_j} (g_{V_k^0 \nu_l \bar{\nu}_l}^L \rightarrow g_{V_k^0 \nu_l \bar{\nu}_l}^R). \tag{19}$$

We note that the form factors follow the relation: $F_{k,L/R}^{\text{Trig}} = F_{1,L/R}^{\text{Trig}} = F_{2,L/R}^{\text{Trig}}$ and $F_{k,R}^{\text{Trig}}|_{V_i, V_j}$ can be obtained directly by replacing $g_{V_k^0 \nu_l \bar{\nu}_l}^L \rightarrow g_{V_k^0 \nu_l \bar{\nu}_l}^R$ in $F_{k,L}^{\text{Trig}}|_{V_i, V_j}$ (as shown in Eq. (19)).

We next take into account the attributions of one-loop triangle graphs which a boson V_i and two charged scalar particles S_j are internal lines (as shown in Fig. 2).

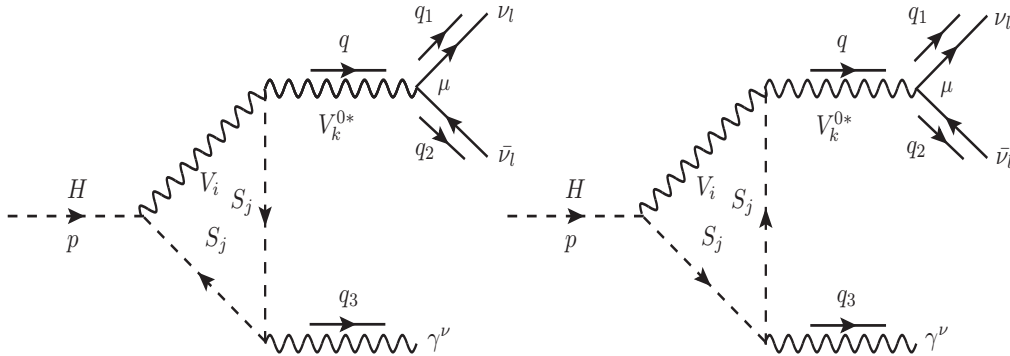


Figure 2: One-loop triangle diagrams with an vector boson V_i and two scalar bosons S_j exchanging in loop.

Applying the same procedure, the form factors read:

$$F_{k,L}^{\text{Trig}}|_{V_i,S_j} = \sum_{V_i,S_j} \frac{eQg_{HV_iS_j} g_{V_k^0 V_i S_j} g_{V_k^0 \nu_l \bar{\nu}_l}^L}{8\pi^2 M_{V_i}^2 (q^2 - M_{V_k^0}^2 + i\Gamma_{V_k^0} M_{V_k^0})} \times \quad (20)$$

$$\times \left\{ (M_{S_j}^2 - M_{V_i}^2 - M_H^2) [C_{22} + C_{12}] (0, q^2, M_H^2, M_{S_j}^2, M_{S_j}^2, M_{V_i}^2) \right. \\ \left. + (M_{S_j}^2 + M_{V_i}^2 - M_H^2) C_2 (0, q^2, M_H^2, M_{S_j}^2, M_{S_j}^2, M_{V_i}^2) \right\},$$

$$F_{k,R}^{\text{Trig}}|_{V_i,S_j} = F_{k,L}^{\text{Trig}}|_{V_i,S_j} (g_{V_k^0 \nu_l \bar{\nu}_l}^L \rightarrow g_{V_k^0 \nu_l \bar{\nu}_l}^R). \quad (21)$$

In addition, we have two vector bosons V_j and a charged scalar S_i exchanging in one-loop triangle diagrams (as described as in Fig. 3). In the same manner as above procedure, the form factors $F_{k,L/R}^{\text{Trig}}$ are presented as functions of PV-coefficients:

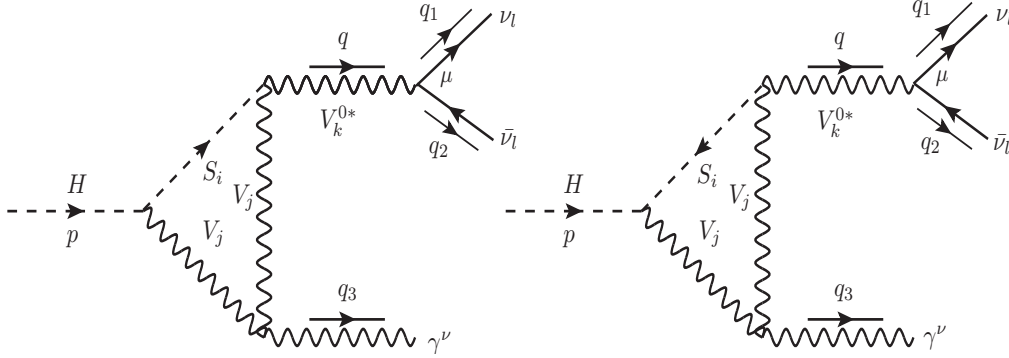


Figure 3: One-loop triangle diagrams with two vector bosons V_j and a scalar boson S_i in loop.

$$F_{k,L}^{\text{Trig}}|_{S_i,V_j} = \sum_{S_i,V_j} \frac{eQg_{HS_iV_j} g_{V_k^0 S_i V_j} g_{V_k^0 \nu_l \bar{\nu}_l}^L}{16\pi^2 M_{V_j}^2 (q^2 - M_{V_k^0}^2 + i\Gamma_{V_k^0} M_{V_k^0})} \times \quad (22)$$

$$\times \left\{ (M_H^2 - M_{S_i}^2 + M_{V_j}^2) [C_{22} + C_{12} + C_2] (0, q^2, M_H^2, M_{V_j}^2, M_{V_j}^2, M_{S_i}^2) \right. \\ \left. + 2M_{V_j}^2 [C_2 + C_0] (0, q^2, M_H^2, M_{V_j}^2, M_{V_j}^2, M_{S_i}^2) \right\},$$

$$F_{k,R}^{\text{Trig}}|_{S_i,V_j} = F_{k,L}^{\text{Trig}}|_{S_i,V_j} (g_{V_k^0 \nu_l \bar{\nu}_l}^L \rightarrow g_{V_k^0 \nu_l \bar{\nu}_l}^R). \quad (23)$$

In further, we also mention the attributions of one-loop bubble and triangle diagrams with both charged scalar bosons S_i, S_j in loop (as depicted in Fig. 4). The resulting for the form factors $F_{k,L/R}^{\text{Trig}}$ read

$$F_{k,L}^{\text{Trig}}|_{S_i,S_j} = \sum_{S_i,S_j} \frac{eQg_{HS_iS_j} g_{V_k^0 S_i S_j} g_{V_k^0 \nu_l \bar{\nu}_l}^L}{4\pi^2 (q^2 - M_{V_k^0}^2 + i\Gamma_{V_k^0} M_{V_k^0})} [C_{22} + C_{12} + C_2] (0, q^2, M_H^2, M_{S_j}^2, M_{S_j}^2, M_{S_i}^2),$$

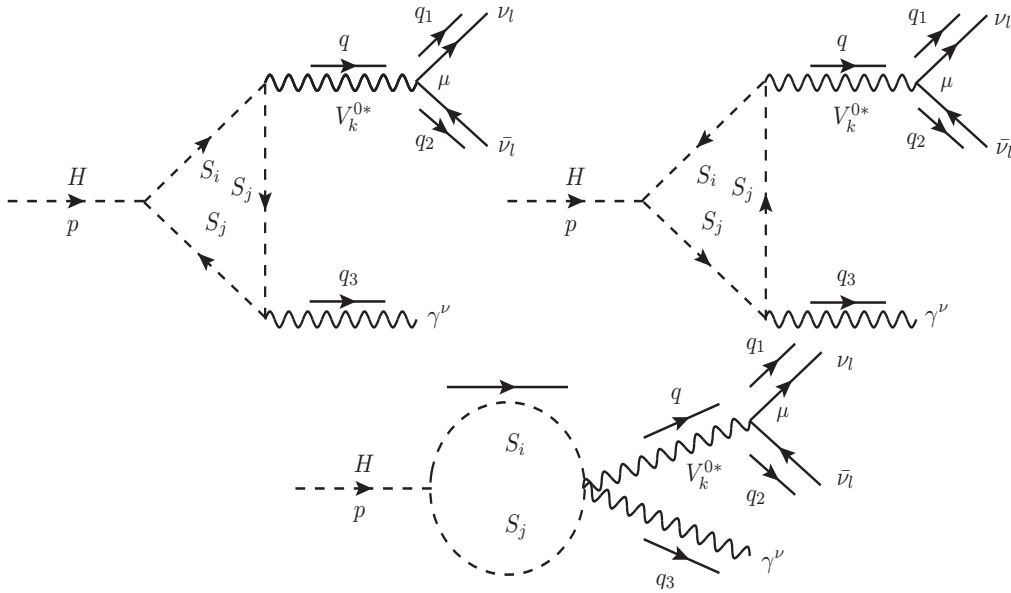


Figure 4: One-loop bubble and triangle diagrams with all charged scalar bosons $S_{i,j}$ internal lines.

$$F_{k,R}^{\text{Trig}}|_{S_i,S_j} = F_{k,L}^{\text{Trig}}|_{S_i,S_j}(g_{V_k^0\nu_l\bar{\nu}_l}^L \rightarrow g_{V_k^0\nu_l\bar{\nu}_l}^R). \quad (24)$$

Lastly, we also have fermions exchanging in the loop of the triangle Feynman diagrams which are depicted as in Fig. 5.

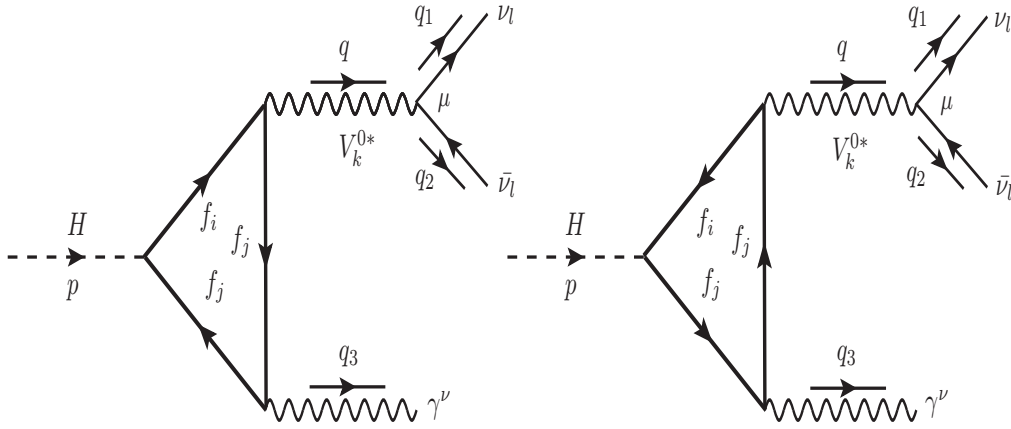


Figure 5: Feynman triangle diagrams with fermion $f_{i/j}$ particles exchanging in loop.

The form factors $F_{k,L/R}^{\text{Trig}}$ for fermion $f_{i/j}$ contributions can be expressed as follows:

$$F_{k,L}^{\text{Trig}}|_{f_i,f_j} = \sum_{f_i,f_j} \frac{eQ_f N_C^f g_{V_k^0\nu_l\bar{\nu}_l}^L}{16\pi^2(q^2 - M_{V_k^0}^2 + i\Gamma_{V_k^0} M_{V_k^0})} (g_{Hf_i f_j L} + g_{Hf_i f_j R})(g_{V_k^0 f_i f_j L} + g_{V_k^0 f_i f_j R}) \times$$

$$\times \left\{ 2(m_{f_i} + m_{f_j}) \left[C_{22} + C_{12} \right] (0, q^2, M_H^2, m_{f_j}^2, m_{f_j}^2, m_{f_i}^2) \right. \quad (26)$$

$$\left. + (m_{f_i} + 3m_{f_j}) C_2(0, q^2, M_H^2, m_{f_j}^2, m_{f_j}^2, m_{f_i}^2) + m_{f_j} C_0(0, q^2, M_H^2, m_{f_j}^2, m_{f_j}^2, m_{f_i}^2) \right\},$$

$$F_{k,R}^{\text{Trig}}|_{f_i, f_j} = F_{k,L}^{\text{Trig}}|_{f_i, f_j} (g_{V_k^0 \nu_l \bar{\nu}_l}^L \rightarrow g_{V_k^0 \nu_l \bar{\nu}_l}^R). \quad (27)$$

2.2.2. One-loop box diagrams

We turn our attention to all one-loop box Feynman diagrams contributing to the decay processes. Firstly, one-loop four-point Feynman diagrams having V_i, V_j in the loop (as described in Fig. 6) are performed. The form factors $F_{k,L/R}^{\text{Box}}$ with $k = 1, 2$ are then given by

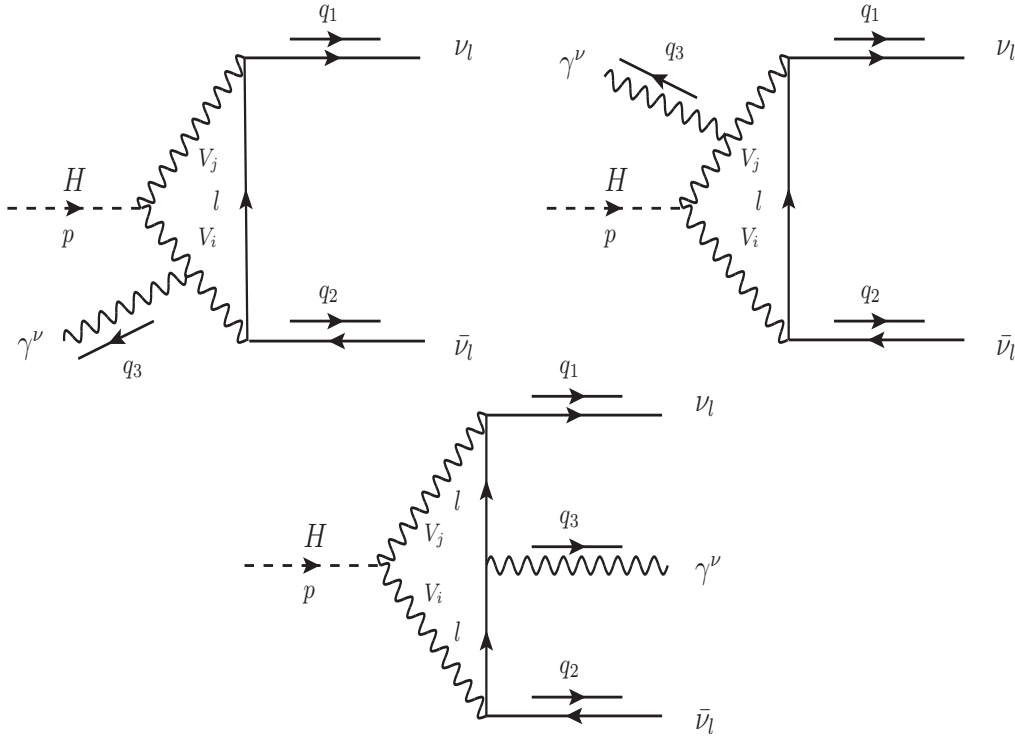


Figure 6: One-loop box diagrams with V_i, V_j exchanging in the loop.

$$F_{1,L}^{\text{Box}}|_{V_i, V_j} = \sum_{V_i, V_j} \frac{eQg_{HV_i V_j} g_{V_i l \nu_l}^L g_{V_j l \nu_l}^L}{16\pi^2 M_{V_i}^2 M_{V_j}^2} \times$$

$$\times \left\{ (M_H^2 + M_{V_i}^2 + M_{V_j}^2) \left[(C_{22} + C_{12})(0, q_{12}, M_H^2, M_{V_i}^2, M_{V_i}^2, M_{V_j}^2) \right. \right.$$

$$\left. + (C_{22} + C_{12})(q_{12}, 0, M_H^2, M_{V_i}^2, M_{V_j}^2, M_{V_j}^2) \right]$$

$$\left. + (M_H^2 + 3M_{V_i}^2 - M_{V_j}^2) \left[C_2(0, q_{12}, M_H^2, M_{V_i}^2, M_{V_i}^2, M_{V_j}^2) \right. \right.$$

$$\begin{aligned}
& +C_2(q_{12}, 0, M_H^2, M_{V_i}^2, M_{V_j}^2, M_{V_j}^2) \Big] \\
& + (2M_{V_i}^2 - 2M_{V_j}^2)C_1(q_{12}, 0, M_H^2, M_{V_i}^2, M_{V_j}^2, M_{V_j}^2) \\
& + 2M_{V_i}^2 \Big[C_0(0, q_{12}, M_H^2, M_{V_i}^2, M_{V_i}^2, M_{V_j}^2) + C_0(q_{12}, 0, M_H^2, M_{V_i}^2, M_{V_j}^2, M_{V_j}^2) \Big] \\
& + m_l^2 \Big[(C_{22} + C_{12} + C_2)(0, 0, q_{13}, m_l^2, m_l^2, M_{V_j}^2) \\
& \quad - (C_{22} + C_{12} + C_2)(0, 0, q_{13}, m_l^2, M_{V_j}^2, M_{V_j}^2) \Big] \\
& + \Big[m_l^2(M_H^2 + M_{V_i}^2 + M_{V_j}^2) + (2d - 4)M_{V_i}^2 M_{V_j}^2 \Big] \times \\
& \times \Big[(D_{33} + D_{23})(0, 0, 0, M_H^2; q_{12}, q_{13}, M_{V_i}^2, m_l^2, M_{V_j}^2, M_{V_j}^2) \\
& \quad + (D_{33} + D_{23} + D_{13})(0, 0, 0, M_H^2; q_{23}, q_{12}, M_{V_i}^2, M_{V_i}^2, m_l^2, M_{V_j}^2) \\
& \quad - (D_{33} + D_{23})(0, 0, 0, M_H^2; q_{23}, q_{13}, M_{V_i}^2, m_l^2, m_l^2, M_{V_j}^2) \Big] \\
& + \Big[m_l^2(M_H^2 + 3M_{V_i}^2 - M_{V_j}^2) + (2d - 8)M_{V_i}^2 M_{V_j}^2 \Big] \times \\
& \quad \times \Big[D_3(0, 0, 0, M_H^2; q_{12}, q_{13}, M_{V_i}^2, m_l^2, M_{V_j}^2, M_{V_j}^2) \\
& \quad + D_3(0, 0, 0, M_H^2; q_{23}, q_{12}, M_{V_i}^2, M_{V_i}^2, m_l^2, M_{V_j}^2) \\
& \quad - D_3(0, 0, 0, M_H^2; q_{23}, q_{13}, M_{V_i}^2, m_l^2, m_l^2, M_{V_j}^2) \Big] \\
& + \Big[2m_l^2(M_{V_i}^2 - M_{V_j}^2) - 4M_{V_i}^2 M_{V_j}^2 \Big] D_2(0, 0, 0, M_H^2; q_{12}, q_{13}, M_{V_i}^2, m_l^2, M_{V_j}^2, M_{V_j}^2) \\
& + 2m_l^2 M_{V_i}^2 \Big[D_0(0, 0, 0, M_H^2; q_{12}, q_{13}, M_{V_i}^2, m_l^2, M_{V_j}^2, M_{V_j}^2) \\
& \quad + D_0(0, 0, 0, M_H^2; q_{23}, q_{12}, M_{V_i}^2, M_{V_i}^2, m_l^2, M_{V_j}^2) \\
& \quad - D_0(0, 0, 0, M_H^2; q_{23}, q_{13}, M_{V_i}^2, m_l^2, m_l^2, M_{V_j}^2) \Big] \Big\},
\end{aligned} \tag{28}$$

$$F_{1,R}^{\text{Box}}|_{V_i, V_j} = F_{1,L}^{\text{Box}}|_{V_i, V_j}(g_{V_i l \nu_l}^L \rightarrow g_{V_i l \nu_l}^R; g_{V_j l \nu_l}^L \rightarrow g_{V_j l \nu_l}^R), \tag{29}$$

$$F_{2,L}^{\text{Box}}|_{V_i, V_j} = F_{1,L}^{\text{Box}}|_{V_i, V_j}(\{q_{13}, q_{23}\} \rightarrow \{q_{23}, q_{13}\}), \tag{30}$$

$$F_{2,R}^{\text{Box}}|_{V_i, V_j} = F_{2,L}^{\text{Box}}|_{V_i, V_j}(g_{V_i l \nu_l}^L \rightarrow g_{V_i l \nu_l}^R; g_{V_j l \nu_l}^L \rightarrow g_{V_j l \nu_l}^R). \tag{31}$$

We find that analytic results for the above form factors are given up to D_{33} -coefficient functions. The reason for that fact can be explained as follows. Although tensor one-loop box integrals with rank $P \geq 4$ appear in each Feynman diagram in Fig. 6, we find that these terms are cancelled out after summing all diagrams. Consequently, the amplitudes are only decomposed up to one-loop box integrals with rank $P = 2$.

We next consider one-loop box diagrams with V_i, S_j in the loop. In order to get the symmetry of $F_{k,L/R}^{\text{Box}}$ which follow the relation

$$F_{1,L/R}^{\text{Box}}|_{V_i, S_j} = F_{2,L/R}^{\text{Box}}|_{V_i, S_j}(\{q_{13}, q_{23}\} \rightarrow \{q_{23}, q_{13}\}), \tag{32}$$

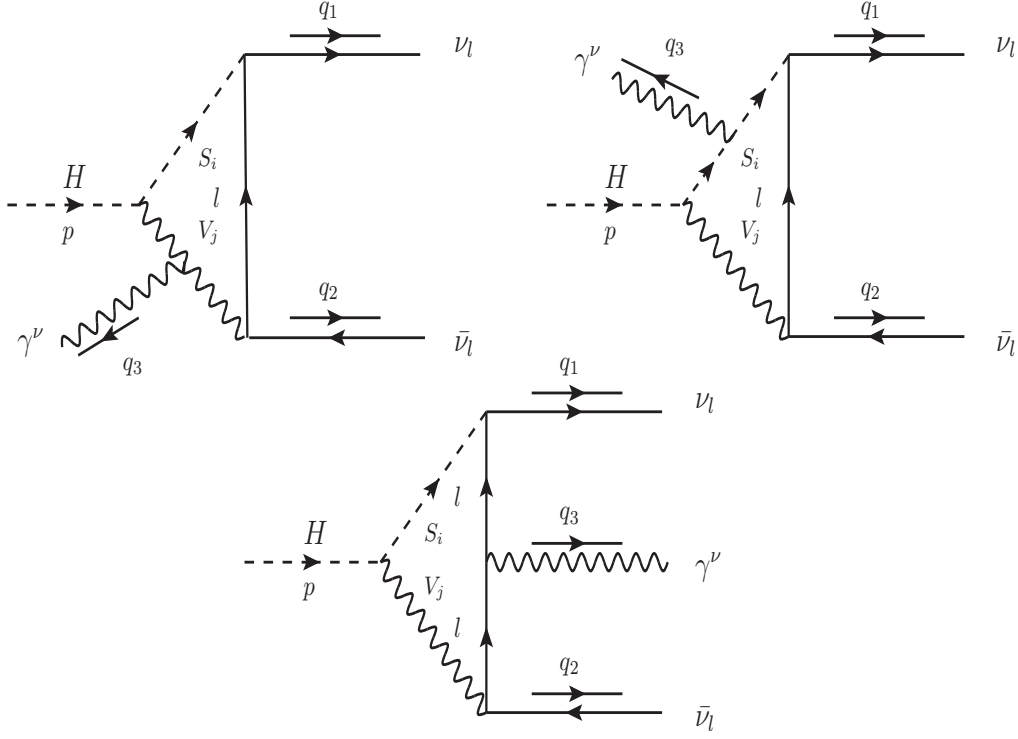


Figure 7: Feynman box diagrams for $V_{i,j}, S_{i,j}$.

we should consider 6 diagrams as shown in Fig. 7 and Fig. 8 together. This is because that the coupling of charged scalar S_i^\pm to $l\bar{\nu}_l$ (and to $\bar{l}\nu_l$) take the different forms (seen Table 2 for more detail). The form factors $F_{k,L/R}^{\text{Box}}$ are then presented as follows:

$$\begin{aligned}
F_{1,L}^{\text{Box}}|_{V_i, S_j} &= \sum_{V_i, S_j} \frac{eQm_l g_{HV_i S_j} g_{S_j l \nu_l}^R g_{V_i l \nu_l}^L}{16\pi^2 M_{V_i}^2} \times \\
&\times \left\{ (M_H^2 - M_{S_j}^2 + M_{V_i}^2) \left[(D_{33} + D_{23} + D_{13})(0, 0, 0, M_H^2; q_{23}, q_{12}, M_{V_i}^2, M_{V_i}^2, m_l^2, M_{S_j}^2) \right. \right. \\
&\quad - (D_{33} + D_{23} + D_{13})(0, 0, 0, M_H^2; q_{23}, q_{12}, M_{S_j}^2, M_{S_j}^2, m_l^2, M_{V_i}^2) \\
&\quad - (D_{33} + D_{23})(0, 0, 0, M_H^2; q_{12}, q_{13}, M_{V_i}^2, m_l^2, M_{S_j}^2, M_{S_j}^2) \\
&\quad + (D_{33} + D_{23})(0, 0, 0, M_H^2; q_{12}, q_{13}, M_{S_j}^2, m_l^2, M_{V_i}^2, M_{V_i}^2) \\
&\quad - (D_{33} + D_{23})(0, 0, 0, M_H^2; q_{23}, q_{13}, M_{V_i}^2, m_l^2, m_l^2, M_{S_j}^2) \\
&\quad \left. - (D_{33} + D_{23})(0, 0, 0, M_H^2; q_{23}, q_{13}, M_{S_j}^2, m_l^2, m_l^2, M_{V_i}^2) \right] \\
&\quad + (M_H^2 - M_{S_j}^2 + 3M_{V_i}^2) \left[D_3(0, 0, 0, M_H^2; q_{23}, q_{12}, M_{V_i}^2, M_{V_i}^2, m_l^2, M_{S_j}^2) \right. \\
&\quad - D_3(0, 0, 0, M_H^2; q_{12}, q_{13}, M_{V_i}^2, m_l^2, M_{S_j}^2, M_{S_j}^2) \\
&\quad \left. - D_3(0, 0, 0, M_H^2; q_{23}, q_{13}, M_{V_i}^2, m_l^2, m_l^2, M_{S_j}^2) \right] \\
&\quad + (M_H^2 - M_{S_j}^2 - M_{V_i}^2) \left[D_3(0, 0, 0, M_H^2; q_{12}, q_{13}, M_{S_j}^2, m_l^2, M_{V_i}^2, M_{V_i}^2) \right. \\
&\quad \left. - D_3(0, 0, 0, M_H^2; q_{23}, q_{12}, M_{S_j}^2, M_{S_j}^2, m_l^2, M_{V_i}^2) \right]
\end{aligned}$$

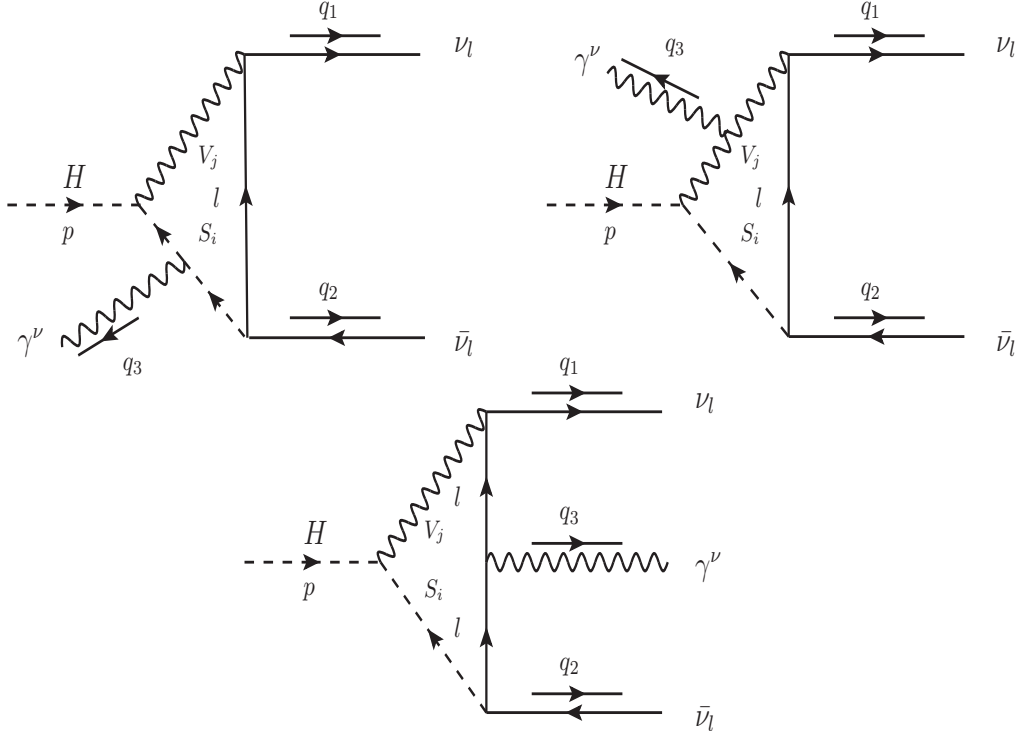


Figure 8: Feynman box diagrams for $V_{i,j}, S_{i,j}$.

$$\begin{aligned}
& -D_3(0, 0, 0, M_H^2; q_{23}, q_{13}, M_{S_j}^2, m_l^2, m_l^2, M_{V_i}^2) \Big] \\
& + 2M_{V_i}^2 \Big[D_0(0, 0, 0, M_H^2; q_{23}, q_{12}, M_{V_i}^2, M_{V_i}^2, m_l^2, M_{S_j}^2) \\
& \quad - D_0(0, 0, 0, M_H^2; q_{23}, q_{13}, M_{V_i}^2, m_l^2, m_l^2, M_{S_j}^2) \\
& \quad - (D_2 + D_0)(0, 0, 0, M_H^2; q_{12}, q_{13}, M_{V_i}^2, m_l^2, M_{S_j}^2, M_{S_j}^2) \\
& \quad - D_2(0, 0, 0, M_H^2; q_{12}, q_{13}, M_{S_j}^2, m_l^2, M_{V_i}^2, M_{V_i}^2) \Big] \\
& - 3 \Big[(C_{22} + C_{12} + C_2)(0, 0, q_{13}, m_l^2, m_l^2, M_{S_j}^2) \\
& \quad + (C_{22} + C_{12} + C_2)(0, 0, q_{13}, m_l^2, M_{S_j}^2, M_{S_j}^2) \Big] \\
& + (C_{22} + C_{12} + C_2)(0, 0, q_{13}, m_l^2, m_l^2, M_{V_i}^2) \\
& - (C_{22} + C_{12} + C_2)(0, 0, q_{13}, m_l^2, M_{V_i}^2, M_{V_i}^2) \Big\},
\end{aligned} \tag{33}$$

$$F_{1,R}^{\text{Box}}|_{V_i, S_j} = F_{1,L}^{\text{Box}}|_{V_i, S_j} (g_{S_j l \nu_l}^R \rightarrow g_{S_j l \nu_l}^L; g_{V_i l \nu_l}^L \rightarrow g_{V_i l \nu_l}^R), \tag{34}$$

$$F_{2,R}^{\text{Box}}|_{V_i, S_j} = F_{2,L}^{\text{Box}}|_{V_i, S_j} (g_{S_j l \nu_l}^R \rightarrow g_{S_j l \nu_l}^L; g_{V_i l \nu_l}^L \rightarrow g_{V_i l \nu_l}^R). \tag{35}$$

In the SM limit, we observe that these contributions are much smaller than other contributions because of the appearance of the factor m_l in Eq. (33). It means that we can take only the τ -lepton contributions for these form factors. But in many BSMs, where new heavy charged leptons with $m_{E_l} \gg m_l$ appear in the loop. These contributions may be significant. For this case, the form factors are obtained directly by replacing l by E_l .

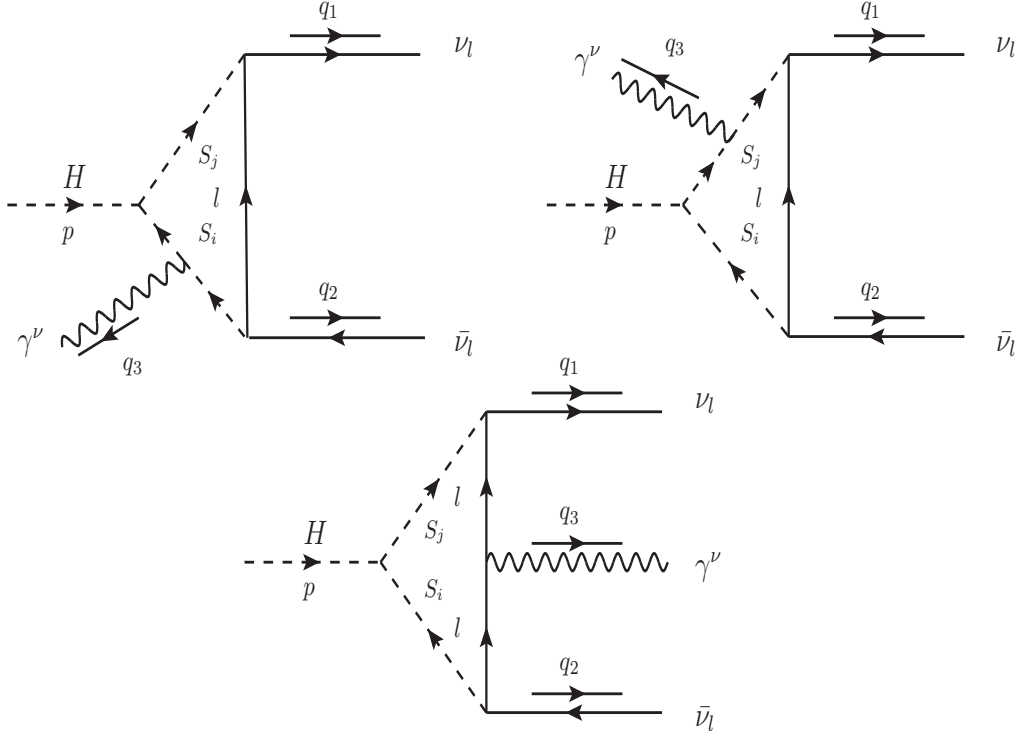


Figure 9: Feynman box diagrams for $V_{i,j}, S_{i,j}$.

We finally end up with the contributions of one-loop box diagrams with scalar charged bosons S_i, S_j in the loop. The corresponding form factors read:

$$\begin{aligned}
F_{1,L}^{\text{Box}}|_{S_i, S_j} &= - \sum_{S_i, S_j} \frac{eQg_{HS_i S_j} g_{S_i l \nu_l}^R g_{S_j l \nu_l}^R}{8\pi^2} \times \\
&\times \left\{ (D_{33} + D_{23} + D_3)(0, 0, 0, M_H^2; q_{12}, q_{13}, M_{S_i}^2, m_l^2, M_{S_j}^2, M_{S_j}^2) \right. \\
&+ (D_{33} + D_{23} + D_{13} + D_3)(0, 0, 0, M_H^2; q_{23}, q_{12}, M_{S_i}^2, M_{S_i}^2, m_l^2, M_{S_j}^2) \\
&\left. + (D_{33} + D_{23} + D_3)(0, 0, 0, M_H^2; q_{23}, q_{13}, M_{S_i}^2, m_l^2, m_l^2, M_{S_j}^2) \right\}, \quad (36)
\end{aligned}$$

$$F_{1,R}^{\text{Box}}|_{S_i, S_j} = F_{1,L}^{\text{Box}}|_{S_i, S_j}(g_{S_i l \nu_l}^R \rightarrow g_{S_i l \nu_l}^L; g_{S_j l \nu_l}^R \rightarrow g_{S_j l \nu_l}^L), \quad (37)$$

$$F_{2,L}^{\text{Box}}|_{S_i, S_j} = F_{1,L}^{\text{Box}}|_{S_i, S_j}(\{q_{13}, q_{23}\} \rightarrow \{q_{23}, q_{13}\}), \quad (38)$$

$$F_{2,R}^{\text{Box}}|_{S_i, S_j} = F_{2,L}^{\text{Box}}|_{S_i, S_j}(g_{S_i l \nu_l}^R \rightarrow g_{S_i l \nu_l}^L; g_{S_j l \nu_l}^R \rightarrow g_{S_j l \nu_l}^L). \quad (39)$$

All the above form factors are checked numerically by verifying ultraviolet finiteness of the results. We find that the results are good stability when varying ultraviolet cutoff parameters. We refer numerical results for this check in appendix A.

Having the correctness form factors for the decay processes, the decay rate is given by [24]:

$$\frac{d\Gamma}{dq_{12}dq_{13}} = \frac{q_{12}}{512\pi^3 M_H^3} \left[q_{13}^2 (|F_{1,R}|^2 + |F_{2,R}|^2) + q_{23}^2 (|F_{1,L}|^2 + |F_{2,L}|^2) \right]. \quad (40)$$

Taking the above integrand over $0 \leq q_{12} \leq M_H^2$ and $0 \leq q_{13} \leq M_H^2 - q_{12}$, one gets the total decay rate. In the next subsection, we show a typical example which we apply the analytic results for

$H \rightarrow \nu_l \bar{\nu}_l \gamma$ in standard model. Phenomenological results for these decay channels also studied with using updated parameters at the LHC.

2.2.3. Standard model case

In this case, we have $V_i, V_j \rightarrow W^+, W^-, V_k^0 \rightarrow Z$. All couplings are replaced by $g_{HV_i V_j} = e M_W / s_W$, $g_{V_k^0 V_i V_j} = e c_W / s_W$, $g_{V_k^0 A V_i V_j} = e^2 c_W / s_W$, $g_{V_k^0 NN}^L = e / (2 s_W c_W)$, $g_{V_k^0 NN}^R = 0$, $g_{H f_i f_j}^L = g_{H f_i f_j}^R = e m_f / (2 s_W M_W)$, $g_{V_k^0 f_i f_j}^L = e (T_3^f - Q_f s_W^2) / (s_W c_W)$, $g_{V_k^0 f_i f_j}^R = -e Q_f s_W / c_W$, $g_{V_i N l}^L = e / (\sqrt{2} s_W)$, $g_{V_i N l}^R = 0$. Analytic results for case of $m_l \rightarrow 0$ are presented as follows:

$$F_{1,L}^{\text{Trig, SM}}|_{W,W} = \frac{\alpha^2}{4 M_W^3 s_W^3 (q^2 - M_Z^2 + i \Gamma_Z M_Z)} \times \quad (41)$$

$$\times \left\{ \left[M_H^2 (2B_{111} + 3B_{11} + B_1) + 2B_{00} + 4B_{001} \right] (M_H^2, M_W^2, M_W^2) \right.$$

$$+ \left[4M_H^2 M_W^2 - 2M_H^2 q^2 + 8(d-1)M_W^4 - 4M_W^2 q^2 \right] \times$$

$$\times \left[C_{22} + C_{12} + C_2 \right] (0, q^2, M_H^2, M_W^2, M_W^2, M_W^2)$$

$$\left. + 4M_W^2 (4M_W^2 - q^2) C_0(0, q^2, M_H^2, M_W^2, M_W^2, M_W^2) \right\},$$

$$F_{1,L}^{\text{Trig, SM}}|_{f,f} = -\frac{\alpha^2 m_f^2 N_C^f Q_f}{2 c_W^2 s_W^3 M_W (q^2 - M_Z^2 + i \Gamma_Z M_Z)} \left(2Q_f s_W^2 - T_3^f \right) \times \quad (42)$$

$$\times \left\{ C_0(0, q^2, M_H^2, m_f^2, m_f^2, m_f^2) + 4 \left[C_{22} + C_{12} + C_2 \right] (0, q^2, M_H^2, m_f^2, m_f^2, m_f^2) \right\}.$$

We also have $F_{k,R}^{\text{Trig, SM}}|_{W,W} = F_{k,R}^{\text{Trig, SM}}|_{f,f} = 0$ for $k = 1, 2$ due to the fact that all couplings g_{\dots}^R are absent in SM. For one-loop box diagrams, the form factors read

$$F_{1,L}^{\text{Box, SM}}|_{W,W} = \frac{\alpha^2}{2 M_W^3 s_W^3} \left\{ (M_H^2 + 2M_W^2) \left[(C_{22} + C_{12} + C_2)(0, q_{12}, M_H^2, M_W^2, M_W^2, M_W^2) \right. \right.$$

$$\left. + (C_{22} + C_{12} + C_2)(q_{12}, 0, M_H^2, M_W^2, M_W^2, M_W^2) \right]$$

$$+ 2(d-2)M_W^4 \left[(D_{33} + D_{23})(0, 0, 0, M_H^2; q_{12}, q_{13}; M_W^2, 0, M_W^2, M_W^2) \right.$$

$$+ (D_{33} + D_{23})(0, 0, 0, M_H^2; q_{23}, q_{13}; M_W^2, 0, 0, M_W^2)$$

$$\left. + (D_{33} + D_{23} + D_{13})(0, 0, 0, M_H^2; q_{23}, q_{12}; M_W^2, M_W^2, 0, M_W^2) \right]$$

$$+ 2(d-4)M_W^4 \left[D_3(0, 0, 0, M_H^2; q_{12}, q_{13}; M_W^2, 0, M_W^2, M_W^2) \right.$$

$$+ D_3(0, 0, 0, M_H^2; q_{23}, q_{12}; M_W^2, M_W^2, 0, M_W^2)$$

$$\left. + D_3(0, 0, 0, M_H^2; q_{23}, q_{13}; M_W^2, 0, 0, M_W^2) \right]$$

$$+ 4M_W^2 \left[C_0(0, q_{12}, M_H^2, M_W^2, M_W^2, M_W^2) \right.$$

$$\left. - M_W^2 D_2(0, 0, 0, M_H^2; q_{12}, q_{13}; M_W^2, 0, M_W^2, M_W^2) \right] \Big\}, \quad (43)$$

$$F_{2,L}^{\text{Box, SM}}|_{W,W} = F_{1,L}^{\text{Box, SM}}|_{W,W} (\{q_{13}, q_{23}\} \rightarrow \{q_{23}, q_{13}\}), \quad (44)$$

$$F_{1,R}^{\text{Box, SM}}|_{W,W} = F_{2,R}^{\text{Box, SM}}|_{W,W} = 0. \quad (45)$$

For phenomenological results, we use following input parameters: $M_Z = 91.1876$ GeV, $\Gamma_Z = 2.4952$ GeV, $M_W = 80.379$ GeV, $M_H = 125.1$ GeV, $m_\tau = 1.77686$ GeV, $m_t = 172.76$ GeV, $m_b = 4.18$ GeV, $m_s = 0.93$ GeV and $m_c = 1.27$ GeV. We first confirm the previous result in Ref. [13] which the decay rate is computed in α -scheme, or $\alpha = 1/137.035999084$. By working in this scheme, the decay rate (for $l = e$) is obtained as $\Gamma_{H \rightarrow \nu_e \bar{\nu}_e \gamma} = 0.480414$ KeV. This value gives a good agreement with the result in Ref. [13].

At the LHC, the decay processes are involved two kind of events: (i) considering photon is undetected we then have Higgs decay to invisible particles; (ii) for detected photon, we observe the Higgs decay to photon plus missing energy. The former events provide important information for controlling SM background for $H \rightarrow \gamma\gamma$ and $H \rightarrow Z\gamma$ which Z may decay to undetected leptons, etc. For latter events, they are interesting for searching dark matter at the LHC. For above reasons, both the events are examined in this paper with using updated parameters at the LHC. In this computation, we work in G_F -scheme which α is evaluated from $G_F = 1.1663787 \times 10^{-5}$ GeV⁻². The resulting reads

$$\alpha^{-1} = \frac{\pi}{\sqrt{2}G_F M_W^2 s_W^2} = 132.184. \quad (46)$$

The new results for decay rates are obtained:

$$\Gamma_{H \rightarrow \nu_l \bar{\nu}_l \gamma}^{\text{Trig}} = 0.536234 \text{ KeV}, \quad (47)$$

$$\Gamma_{H \rightarrow \nu_l \bar{\nu}_l \gamma}^{\text{Tot}} = 0.554933 \text{ KeV}. \quad (48)$$

We realize that the attributions of $|F_{k/L(R)}^{\text{Box}}|^2$ is much smaller than the other terms. Differential decay rate is also plotted as function of invariant mass of $m_{\nu_l \bar{\nu}_l}$ (or $m_{\nu_l \bar{\nu}_l} = \sqrt{q_{12}}$). The distribution is defined in form of:

$$\frac{d\Gamma}{dm_{\nu_l \bar{\nu}_l}} = \frac{m_{\nu_l \bar{\nu}_l}^3}{512\pi^3 M_H^3} \int_0^{M_H^2 - 2m_{\nu_l \bar{\nu}_l}^2} dq_{13} \left[q_{13}^2 (|F_{1,R}|^2 + |F_{2,R}|^2) + q_{23}^2 (|F_{1,L}|^2 + |F_{2,L}|^2) \right]. \quad (49)$$

The distribution is shown in Fig. 10. We observe a peak of $Z^* \rightarrow \nu_l \bar{\nu}_l$ which is around M_Z . In the region $m_{\nu \bar{\nu}} \leq M_Z$, the contributions of box diagrams are visible. While they give a small contribution beyond the peak.

We are also interested in the case of photon that can be tested at the colliders. In this case, one should apply the energy cuts for final photon. The results are shown with different cuts for photon in Table 1. The updated results are important should take into account at the HL-LHC and future colliders.

We note that all numerical results shown in this subsection are for a family of neutrino in final state. For all neutrinos, we multiply factor 3 for all above results.

3. Conclusions

We have presented analytic formulas for all possible one-loop contributions to the SM-like Higgs decay $H \rightarrow \nu_l \bar{\nu}_l \gamma$ that are valid in many BSMs. Additional vector bosons, charged fermions and charged (and also neutral) scalar particles exchanging in the loop diagrams have considered in this computation. General statement, we conclude that the evaluations can be extended directly for general numbers of the extra neutrinos in final states. Analytic results are expressed

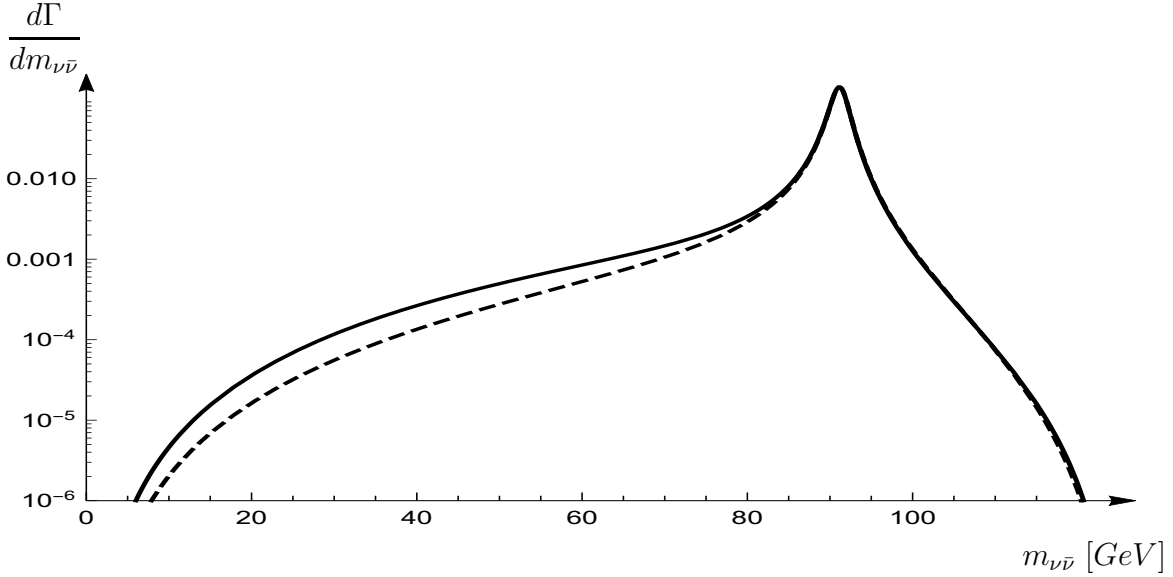


Figure 10: Differential decay rate is plotted as function of invariant mass of $m_{\nu_l \bar{\nu}_l}$.

Γ [KeV]/ E_γ^{cut} [GeV]	5	30	50
$\Gamma_{H \rightarrow \gamma \nu_l \bar{\nu}_l}^{\text{Trig}}$	0.536232	0.188952	0.00529925
$\Gamma_{H \rightarrow \gamma \nu_l \bar{\nu}_l}^{\text{Total}}$	0.554931	0.20927	0.00993683

Table 1: Decay widths in the case of photon that can be tested.

in a general form which written in terms of Passarino-Veltman scalar functions that can be evaluated numerically using `LoopTools`. The computations have checked numerically by verifying ultraviolet finiteness of the results. We find that the results are good stability when varying ultraviolet cutoff parameters. We then apply the results to the standard model which the decay rates are generated and cross-checked to previous computation. All physical results for the decay channels within standard model are studied with the updated input parameters at the Large Hadron Collider.

Acknowledgment: This research is funded by Vietnam National Foundation for Science and Technology Development (NAFOSTED) under the grant number No.103.01-2019.387.

Appendix A. Numerical checks for the calculations

Numerical checks for the computations are performed for all the above form factors. The results must be independent of ultraviolet cutoff ($C_{UV} = 1/\varepsilon$) and μ^2 parameters. For demonstrating, we take the form factors $F_{1L}^{\text{Trig}}|_{WW}$ and $F_{1L}^{\text{Box}}|_{WW}$, appear high rank tensor one-loop integrals in the amplitude, as typical examples. Numerical results are presented at arbitrary sampling point in physical region.

Diagrams /(C_{UV}, μ^2)	(0, 1)	($10^5, 10^7$)
<i>1st</i>	$5.684478386592405 \cdot 10^{-8}$ $+ 7.556282593901243 \cdot 10^{-8} i$	-0.0004193697635384515 $-0.0005574612531042949 i$
<i>2nd</i>	$5.684478386592405 \cdot 10^{-8}$ $+ 7.556282593901243 \cdot 10^{-8} i$	-0.0004193697635384515 $-0.0005574612531042948 i$
<i>3rd</i>	$-6.951714952517838 \cdot 10^{-8}$ $-9.24079908850924 \cdot 10^{-8} i$	0.00083878369949511 $+ 0.0011149812238695827 i$
Sum	$4.417241820666968 \cdot 10^{-8}$ $+5.871766099293248 \cdot 10^{-8} i$	$4.417241820666968 \cdot 10^{-8}$ $+5.871766099293248 \cdot 10^{-8} i$

Table A.2: Numerical checks for $F_{1L}^{\text{Trig}}|_{WW}$.

Diagrams /(C_{UV}, μ^2)	(0, 1)	($10^5, 10^7$)
<i>1st</i>	$-3.114167099931247 \cdot 10^{-10}$	$-3.114167099931247 \cdot 10^{-10}$
<i>2nd</i>	$6.440660243424821 \cdot 10^{-10}$	$6.440660243424821 \cdot 10^{-10}$
<i>3rd</i>	$-9.02406987251144 \cdot 10^{-11}$	$-9.02406987251144 \cdot 10^{-11}$
Sum	$2.424086156242413 \cdot 10^{-10}$	$2.424086156242413 \cdot 10^{-10}$

Table A.3: Numerical checks for $F_{1L}^{\text{Box}}|_{WW}$.

Appendix B. Feynman rules

References

- [1] A. Liss *et al.* [ATLAS], [[arXiv:1307.7292](#)] [hep-ex].
- [2] [CMS], [[arXiv:1307.7135](#)] [hep-ex].
- [3] H. Baer, T. Barklow, K. Fujii, Y. Gao, A. Hoang, S. Kanemura, J. List, H. E. Logan, A. Nomerotski and M. Perelstein, *et al.* [[arXiv:1306.6352](#)] [hep-ph].
- [4] A. M. Sirunyan *et al.* [CMS], Phys. Lett. B **793** (2019), 520-551

Particle types	Propagators
Fermions f	$i \frac{\not{k} + m_f}{k^2 - m_f^2}$
Gauge boson V_i	$\frac{-i}{p^2 - M_{V_i}^2} \left(g^{\mu\nu} - \frac{p^\mu p^\nu}{M_{V_i}^2} \right)$
Gauge boson V_k^0	$\frac{-i}{p^2 - M_{V_k^0}^2 + i\Gamma_{V_k^0} M_{V_k^0}} \left(g^{\mu\nu} - \frac{p^\mu p^\nu}{M_{V_k^0}^2} \right)$
Charged (neutral) scalar bosons $S_i(S_k^0)$	$\frac{i}{p^2 - M_{S_i}^2 (M_{S_k^0}^2)}$

Table B.4: Feynman rules involving the decay in unitary gauge.

- [5] M. Aaboud *et al.* [ATLAS], Phys. Rev. Lett. **122** (2019) no.23, 231801
- [6] M. Aaboud *et al.* [ATLAS], Phys. Lett. B **793** (2019), 499-519
- [7] V. S. Ngairangbam, A. Bhardwaj, P. Konar and A. K. Nayak, Eur. Phys. J. C **80** (2020) no.11, 1055
- [8] G. Aad *et al.* [ATLAS], Eur. Phys. J. C **72** (2012), 1844
- [9] G. Belanger, B. Dumont, U. Ellwanger, J. F. Gunion and S. Kraml, Phys. Lett. B **723** (2013), 340-347
- [10] M. Heikinheimo, K. Tuominen and J. Virkajarvi, JHEP **07** (2012), 117
- [11] A. M. Sirunyan *et al.* [CMS], JHEP **10** (2019), 139.
- [12] A. M. Sirunyan *et al.* [CMS], JHEP **03** (2021), 011
- [13] Y. Sun and D. N. Gao, Phys. Rev. D **89** (2014) no.1, 017301
- [14] J. F. Kamenik and C. Smith, Phys. Rev. D **85** (2012), 093017
doi:10.1103/PhysRevD.85.093017
- [15] H. Davoudiasl, H. S. Lee, I. Lewis and W. J. Marciano, Phys. Rev. D **88** (2013) no.1, 015022
- [16] D. Curtin, R. Essig, S. Gori, P. Jaiswal, A. Katz, T. Liu, Z. Liu, D. McKeen, J. Shelton and M. Strassler, *et al.* Phys. Rev. D **90** (2014) no.7, 075004
- [17] C. Petersson, A. Romagnoni and R. Torre, JHEP **10** (2012), 016
- [18] A. Denner and S. Dittmaier, Nucl. Phys. B **734** (2006), 62-115
- [19] H. H. Patel, Comput. Phys. Commun. **197** (2015), 276-290
- [20] T. Hahn and M. Perez-Victoria, Comput. Phys. Commun. **118** (1999), 153-165.

Vertices	Couplings
$H \cdot \bar{f}_i \cdot f_j$	$-i \left(g_{Hf_i f_j}^L P_L + g_{Hf_i f_j}^R P_R \right)$
$H \cdot V_i^\mu \cdot V_j^\nu$	$i g_{HV_i V_j} g^{\mu\nu}$
$H \cdot S_i \cdot S_j$	$-i g_{HS_i S_j}$
$H(p) \cdot V_i^\mu \cdot S_j(q)$	$i g_{HV_i S_j} (p - q)^\mu$
$A^\mu \cdot f_i \cdot \bar{f}_i$	$ieQ_f \gamma^\mu$
$A^\mu(p_1) \cdot V_i^{Q\nu}(p_2) \cdot V_i^{-Q\lambda}(p_3)$	$-ieQ \Gamma^{\mu\nu\lambda}(p_1, p_2, p_3)$
$A^\mu \cdot S_i^Q(p) \cdot S_i^{-Q}(q)$	$ieQ (p - q)^\mu$
$V_k^{0\mu} \cdot f_i \cdot \bar{f}_j$	$i\gamma^\mu \left(g_{V_k^0 f_i f_j}^L P_L + g_{V_k^0 f_i f_j}^R P_R \right)$
$V_k^{0\mu}(p_1) \cdot V_i^\nu(p_2) \cdot V_j^\lambda(p_3)$	$-i g_{V_k^0 V_i V_j} \Gamma^{\mu\nu\lambda}(p_1, p_2, p_3)$
$V_k^{0\mu} \cdot S_i(p) \cdot S_j(q)$	$i g_{V_k^0 S_i S_j} (p - q)^\mu$
$V_k^{0\mu} \cdot V_i^\nu \cdot S_j$	$g_{V_k^0 V_i S_j} g^{\mu\nu}$
$V_i^\mu \cdot \bar{l} \cdot \nu_l$	$i\gamma^\mu \left(g_{V_i l \nu_l}^L P_L + g_{V_i l \nu_l}^R P_R \right)$
$S_i \cdot \bar{l} \cdot \nu_l$	$ig_{S_i l \nu_l}^L P_L + ig_{S_i l \nu_l}^R P_R$
$S_i^* \cdot l \cdot \bar{\nu}_l$	$ig_{S_i l \nu_l}^R P_L + ig_{S_i l \nu_l}^L P_R$
$V_k^{0\mu} \cdot A^\nu \cdot V_i^\alpha \cdot V_j^\beta$	$-i g_{V_k^0 AV_i V_j} S^{\mu\nu, \alpha\beta}$

Table B.5: Feynman couplings in the unitary gauge with $P_{L/R} = (1 \mp \gamma_5)/2$, $\Gamma^{\mu\nu\lambda}(p_1, p_2, p_3) = g^{\mu\nu}(p_1 - p_2)^\lambda + g^{\lambda\nu}(p_2 - p_3)^\mu + g^{\mu\lambda}(p_3 - p_1)^\nu$ and $S^{\mu\nu, \alpha\beta} = 2g^{\mu\nu}g^{\alpha\beta} - g^{\mu\alpha}g^{\nu\beta} - g^{\mu\beta}g^{\nu\alpha}$ and Q denotes the electric charge of the gauge and charged bosons V_i^Q and S^Q . When we consider the extra charged leptons E_l in the loop, the results will be obtained directly by replacing l by E_l respectively.

- [21] A. Kachanovich, U. Nierste and I. Nišandžić, Phys. Rev. D **101** (2020) no.7, 073003.
- [22] L. B. Chen, C. F. Qiao and R. L. Zhu, Phys. Lett. B **726** (2013), 306-311.
- [23] D. A. Dicus and W. W. Repko, Phys. Rev. D **87** (2013) no.7, 077301.
- [24] A. Kachanovich, U. Nierste and I. Nišandžić, Phys. Rev. D **101** (2020) no.7, 073003.
- [25] G. Aad *et al.* [ATLAS], Phys. Lett. B **819** (2021), 136412.

- [26] A. M. Sirunyan *et al.* [CMS], JHEP **11** (2018), 152
- [27] J. C. Pati and A. Salam, Phys. Rev. D **10**, 275-289 (1974) [erratum: Phys. Rev. D **11**, 703-703 (1975)].
- [28] R. N. Mohapatra and J. C. Pati, Phys. Rev. D **11**, 2558 (1975).
- [29] G. Senjanovic and R. N. Mohapatra, Phys. Rev. D **12**, 1502 (1975).
- [30] M. Singer, J. W. F. Valle and J. Schechter, Phys. Rev. D **22**, 738 (1980).
- [31] J. W. F. Valle and M. Singer, Phys. Rev. D **28**, 540 (1983).
- [32] F. Pisano and V. Pleitez, Phys. Rev. D **46**, 410-417 (1992).
- [33] P. H. Frampton, Phys. Rev. Lett. **69**, 2889-2891 (1992).
- [34] R. A. Diaz, R. Martinez and F. Ochoa, Phys. Rev. D **72**, 035018 (2005).
- [35] R. M. Fonseca and M. Hirsch, JHEP **08** (2016), 003
- [36] R. Foot, H. N. Long and T. A. Tran, Phys. Rev. D **50**, no.1, R34-R38 (1994).
- [37] L. A. Sanchez, F. A. Perez and W. A. Ponce, Eur. Phys. J. C **35** (2004), 259-265 [[arXiv:hep-ph/0404005](#) [hep-ph]].
- [38] W. A. Ponce and L. A. Sanchez, Mod. Phys. Lett. A **22** (2007), 435-448 [[arXiv:hep-ph/0607175](#) [hep-ph]].
- [39] Riazuddin and Fayyazuddin, Eur. Phys. J. C **56** (2008), 389-394 [[arXiv:0803.4267](#) [hep-ph]].
- [40] A. Jaramillo and L. A. Sanchez, Phys. Rev. D **84** (2011), 115001 [[arXiv:1110.3363](#) [hep-ph]].
- [41] H. N. Long, L. T. Hue and D. V. Loi, Phys. Rev. D **94** (2016) no.1, 015007 [[arXiv:1605.07835](#) [hep-ph]].

